Available online at www.sciencedirect.com

ScienceDirect

Procedia Structural Integrity 64 (2024) 2083–2090

Structural Integrity Procedia

www.elsevier.com/locate/procedia

SMAR 2024 – 7th International Conference on Smart Monitoring, Assessment and Rehabilitation of Civil Structures

Development and characterization of thin iron-based shape memory alloy prestressing wire

Zafiris Triantafyllidis[a]*, Meet Jaydeepkumar Oza[a,b], Julien Michels[c], Mateusz Wyrzykowski[a], Moslem Shahverdi[a,d]

[a]*Empa, Swiss Federal Laboratories for Materials Science and Technology, Überlandstrasse 129, 8600 Dübendorf, Switzerland*
[b]*Laboratory for Photonic Materials and Characterization, École Polytechnique Fédérale de Lausanne (EPFL), Lausanne, 1015, Switzerland*
[c]*re-fer AG, Riedmattli 9, 6423 Seewen, Switzerland*
[d]*School of Civil Engineering, University of Tehran, Tehran 4563-11155, Iran*

Abstract

Iron-based shape memory alloys (Fe-SMA) have been used successfully in the previous years as prestressing reinforcement in the form of rebars, rods and flat strips, for various types of structural elements and loading scenarios. This paper introduces a new application of this material in the form of thin wire. An experimental characterization study is presented herein for Fe-SMA wire that was drawn to a diameter of 0.5 mm, regarding its tensile stress-strain response and recovery stress development upon heating, for different activation temperatures and prestraining levels. Furthermore, an investigation is presented regarding the effects of heat treatment conditions on the mechanical response and prestressing performance of the wire. For the optimum heat treatment conditions and activation temperature range considered in this study, the measured tensile strength and recovery stress of the Fe-SMA wire was 1117 MPa and up to 390 MPa, respectively. The results indicate a strong potential of Fe-SMA as a candidate prestressing material where flexible wire cross-sections of small diameter are desired instead of larger, solid cross-section tendons (e.g., multi-strand wire ropes or concrete confinement spirals), or as novel short fiber reinforcement for concrete with prestressing capabilities.

Keywords: Iron-based shape memory alloy; Fe-SMA prestressing; wire; recovery stress

* Corresponding author. Tel.: +41 58 765 4802; fax: +41 58 765 6955.
E-mail address: Zafeirios.Triantafyllidis@empa.ch

10.1016/j.prostr.2024.09.304

1. Introduction: Shape memory alloy wire applications in structural engineering

Shape memory alloys (SMA) have found a broad range of commercial applications in the aerospace, automotive, biomedical, and other industries since the discovery of shape memory effect in nickel-titanium (NiTi) alloy in the 1960s. Owing to their remarkable ability to change shape upon heating and their pseudoelastic behavior, SMAs have been used widely in the form of wires and thin strips as active materials for actuation and smart sensing structures, as well as in applications requiring energy absorption, vibration damping and high recoverable deformation capacity (Kumar & Lagoudas, 2008). The beneficial characteristics of shape memory and pseudoelasticity of SMAs were introduced in structural engineering relatively recently (practically, since the beginning of this century), and have been successfully used in prestressing reinforcement for concrete & steel structures and in self-centering reinforcement/devices for crack recovery and damage mitigation (Raza et al., 2022; Wang et al., 2023).

SMA wires were first introduced in structural engineering research as a means of studying the feasibility of prestressing concrete by triggering the reversible martensitic transformation in prestrained embedded wires via heating to generate recovery stresses, and thus transfer a prestressing force to the concrete element. The feasibility of prestressing small-scale concrete beams or plates to reduce deflections and close cracks was demonstrated in studies exploiting individual NiTi wires with diameters of ⌀2.0-3.5 mm (Krstulovic-Opara & Naaman, 2000; Deng et al., 2006; Li et al., 2006) and twisted 4-wire strands made of ⌀0.64 mm NiTi wires (Maji & Negret, 1998). Despite the fact that wire geometries are practical for experimental studies in the small scale, these are not efficient as primary prestressing reinforcement in real-scale structures, in which larger tendon cross-sections are necessary to develop the required prestress. Larger diameter multi-strand superelastic SMA cables have also been developed though from NiTi wires (Reedlunn et al., 2013; Ozbulut et al., 2016), and have been used as tensile reinforcement in concrete beams (Mas et al., 2017). However, the low modulus of elasticity of NiTi-based alloys can be a limiting factor resulting in considerably lower flexural rigidity of the beams compared to counterparts with steel rebars (Mas et al., 2017). Nowadays, after the development and introduction of cost-effective iron-based shape memory alloys (Fe-SMA), a large variety of commercial prestressing tendons in the form of solid rods, rebars, plates and strips are available for structural elements, which can be effectively applied as internal reinforcement or externally applied strengthening. A comprehensive review on those is given by Raza et al. (2022).

A practical application for flexible SMA wires as load bearing elements in concrete structures is continuous spiral reinforcement. Mas et al. (2016) used continuous ⌀3 mm NiTi wire spirals to reinforce shear-critical concrete beams, demonstrating superior ductility in shear compared to beams with conventional steel stirrups due to the pseudoelasticity of NiTi. Rius et al. (2019) considered ⌀3 mm NiTiNb wires wrapped externally around shear critical concrete beams, as a method of active shear strengthening by applying transverse prestress via shape recovery of the spirals. Another very promising application of SMA wire spirals is active confinement of concrete. Several researchers demonstrated the efficiency of continuous NiTi and NiTiNb wires as transverse prestressing wraps for enhancing the strength and deformation capacity of axially loaded concrete cylinders (Krstulovic-Opara & Thiedeman, 2000; Shin & Andrawes, 2010; Choi et al., 2010; Gholampour & Ozbakkaloglu, 2018), as well as the rotation capacity of reinforced concrete columns under cyclic lateral loading (Shin & Andrawes, 2011; Choi et al., 2012).

Finally, thin SMA wires were used to produce short fiber reinforcement for concrete. Moser et al. (2005) proved the feasibility of applying prestress in small mortar prisms that contained layers of planar NiTi fiber loops of ⌀0.25 mm with a fiber content of 1.2%, which were activated upon heating of the hardened prisms. Lee et al. (2018a; 2018b) explored the crack closure performance of randomly dispersed and unidirectional straight fibers embedded in cementitious mortars. These authors used ⌀0.67mm NiTi and NiTiNb wires at different fiber contents in small prisms that were pre-cracked and subsequently heated to trigger shape recovery, and thereby recover the opened cracks through the prestress developed by the fibers. In addition, several authors examined the enhancements in crack recovery, re-centering performance and energy dissipation in fiber-reinforced concrete prisms subjected to cyclic flexural loading, using twisted-strand (7× ⌀0.117mm) fibers of superelastic NiTi (Sherif et al., 2017), single-hooked superelastic NiTi fibers of ⌀0.75 mm (Aslani et al., 2019), and double-hooked superelastic NiTi fibers of ⌀1.0 mm (Menna et al., 2023).

2. Development of a Fe-SMA wire for prestressing applications

All of the studies identified in the previous section concerning SMA wires were conducted using NiTi-based alloys. In addition to their remarkable shape recovery and pseudoelastic characteristics, a practical reality leading to the implementation of NiTi-based alloys compared to other SMA compositions is that these are readily available in commercial wire products, since they are already used in other industries for actuation and sensing. However, their high material cost and low modulus of elasticity compared to conventional steel wires and fiber reinforcements are hindering their wider implementation in structural applications, despite the benefits of shape memory and pseudoelasticity. In this respect, the low-cost and higher modulus Fe-SMA has been proven very effective as prestressing tendons in a wide range of structural applications, with numerous successful field applications to date (Raza et al., 2022). Therefore, there is high potential for Fe-SMA as a candidate material for wire geometries as an alternative to NiTi-based alloys for the above-mentioned applications.

This paper considers the shape memory alloy with composition Fe-17Mn-5Si-10Cr-4Ni-1(V,C) (mass%) that was developed at Empa (Dong et al., 2009) and is commercialized by re-fer AG as memory®-steel. An experimental batch of wire was cold-drawn from coiled smooth Fe-SMA rebar to a diameter of 0.5 mm (Fig. 1); this was chosen for investigation as a representative mid-range diameter based on the previous studies regarding NiTi-based wires and fibers, as well as a mid-range value of the typical diameters used in steel fiber-reinforced and ultra-high performance concrete. The following section presents the results of an experimental campaign for the characterization of the new Fe-SMA wire with respect to its monotonic tensile stress-strain characteristics and recovery stress development upon shape memory activation, including an initial investigation regarding heat treatment conditions to improve the mechanical response of the wire after the cold-drawing process.

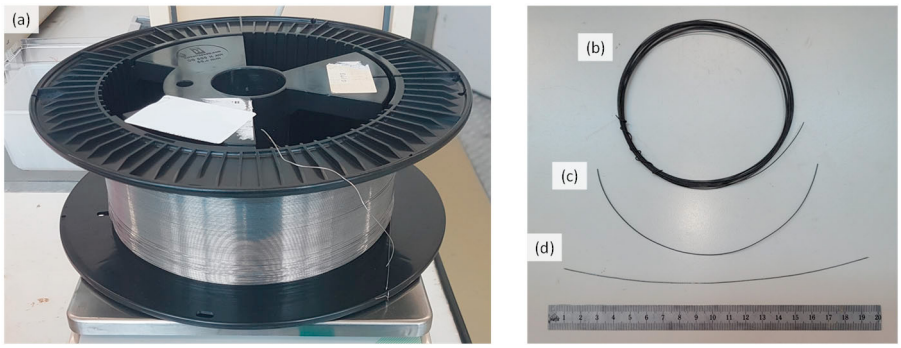

Fig. 1. (a) Fe-SMA wire spool in the as-received condition; (b) cut-out coil for heat treatment; (c) cut-out & (d) straightened tensile specimen.

3. Mechanical characterization

3.1. Specimen preparation

The tensile stress-strain characteristics and recovery stress development of the Fe-SMA wire were determined from specimens that were cut out at random locations across the length of the continuous spool (Fig. 1). Initial testing of specimens in the as-received condition revealed a high level of strain hardening imposed on the material from the wire drawing process, resulting in a significant increase in tensile strength but also very limited ductility and low recovery stress. Therefore, shorter coils of 2 m length were cut out (Fig. 1(b)) and were heated in an electric furnace to anneal the wire and improve its ductility and shape memory characteristics. Individual specimens of the as-received condition were randomly obtained between the extracted coils for annealing, to verify the uniformity of the as-received mechanical properties as well as the diameter (0.5 ± 0.001 mm) across the spool length. The shorter coils for annealing had a diameter of approximately 100-120mm, which resulted naturally during uncoiling from the initial plastic spool (Fig. 1(a)), due to residual stresses from the rolling and spooling processes after drawing.

Specimens for tensile testing and activation were cut out (Fig. 1(c)) and straightened gently by hand (Fig. 1(d)), so that they can be aligned and gripped in the universal testing machine without eccentricity.

The heat treatment conditions were selected based on the work of Yang et al. (2021) regarding hot-rolled plates of the same Fe-SMA composition as considered herein. The wire coils were solution-treated in an electric furnace without protective atmosphere at a temperature of 1070ºC for 2 hours. According to Yang et al. (2021) this solution temperature and duration is optimal for dissolving residual precipitates in the alloy microstructure while preventing austenite grain growth, which occurs at temperatures above 1070ºC. After the 2-hour heating duration, the wires were quenched in water to avoid precipitate formation during the cooling stage (Yang et al., 2021). A secondary ageing heat treatment step followed upon cooling down to improve the microstructure and increase the obtained recovery stress (Yang et al., 2021), considering two different trial conditions: (i) 1 hour of heating at 700ºC and (ii) 24 hours at 600ºC, both followed by natural cooling in air.

In addition, the study presented herein considered the effect of varying the annealing temperature in an attempt to find an optimum combination between strength reduction and ductility enhancement during the recovery and recrystallization stages of the annealing process. Thus, except for the optimal solution treatment of 2 hours at 1070ºC, the experimental campaign considered reducing the annealing temperature from 1000ºC to 800ºC at increments of 50ºC and keeping the same heating duration of 2 hours, but without any additional ageing step.

3.2. Tensile testing

Tests were performed in a Zwick/Roell Z020 electromechanical machine fitted with a 2.5 kN load cell. The specimens were fixed with screw-type flat serrated grips (Fig. 2 (a)); the free length of the wire was 80 mm and the gripped length was 50 mm. Strain was measured with an automatic extensometer with feeler arms at a gauge length of 40 mm. The specimens were loaded monotonically to failure at a crosshead displacement rate of 2 mm/min. At least three specimens were tested for each wire condition to assess repeatability. Fig. 2(b) shows the obtained stress-strain responses for all of the examined wire conditions. The response of the original Fe-SMA coiled bar, from which the wire was drawn, is also shown for comparison. Table 1 provides the measured properties in terms of the 0.1% and 0.2% offset yield (proof) stress, tensile strength, ultimate tensile strain, and elastic modulus. Please note that the modulus values are only indicative, because the measurements were based on different stress ranges between different wire types. These were measured by linear fitting generally in the stress range of 100-300 MPa for wires treated at lower temperatures, and 50-150MPa for the higher temperatures, due to the differences in the effective strain range where linearity is observed for different treatments. However, these ranges had to be adjusted for some individual specimens, due to the presence of more pronounced toes at the beginning of the obtained stress-strain curves, arising from the initial curvature of the wires.

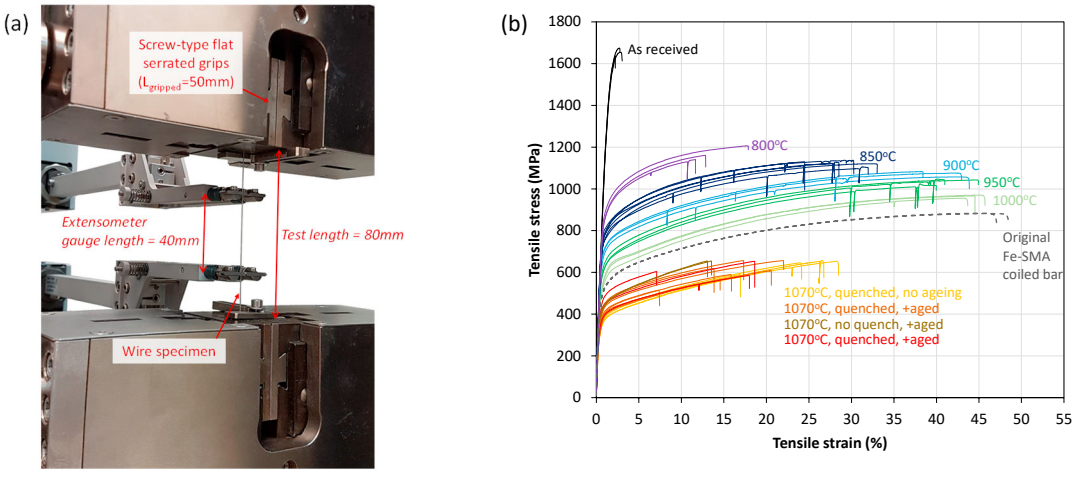

Fig. 2. (a) Wire testing setup; (b) ambient temperature stress-strain response of ⌀0.5mm Fe-SMA wire at various solution treatment conditions.

Table 1. Measured tensile properties of Fe-SMA wire at different heat treatment conditions (mean values ± standard deviation).

Condition	Elastic modulus (GPa)	0.1% Proof stress (MPa)	0.2% Proof stress (MPa)	Tensile strength (MPa)	Ult. tensile strain (%)
Initial Fe-SMA bar	170.1 ± 2.6	407.8 ± 6.9	450.1 ± 5.4	882.2 ± 1.2	47.89 ± 1.00
As-received wire	133.2 ± 3.4	1024.0 ± 41.3	1233.1 ± 35.4	1655.3 ± 18.5	2.67 ± 0.41
1070ºC	123.9 ± 19.0	280.2 ± 15.0	317.2 ± 13.2	639.8 ± 28.5	24.84 ± 4.71
1070ºC, aged 1hr 700ºC	142.4 ± 27.4	320.8 ± 26.7	364.3 ± 29.5	602.0 ± 39.9	13.96 ± 4.96
1070ºC, air cooled (no quench), aged 1hr 700ºC	157.5 ± 11.0	337.9 ± 17.0	370.4 ± 21.3	645.6 ± 15.4	14.74 ± 2.48
1070ºC, aged 24hr 600ºC	140.2 ± 0.7	353.8 ± 53.4	385.9 ± 45.9	614.0 ± 35.2	14.63 ± 6.42
1000ºC	174.8 ± 23.0	411.6 ± 11.1	469.6 ± 7.0	864.2 ± 20.6	44.65 ± 1.01
950ºC	167.8 ± 6.5	484.7 ± 10.7	547.2 ± 4.8	1038.6 ± 13.3	42.70 ± 2.51
900ºC	167.5 ± 14.4	559.1 ± 19.3	631.3 ± 13.4	1071.6 ± 13.0	41.76 ± 2.93
850ºC	171.4 ± 4.4	576.6 ± 36.6	680.4 ± 22.5	1116.6 ± 10.5	28.76 ± 2.92
800ºC	159.8 ± 16.0	689.3 ± 27.2	783.8 ± 22.2	1168.8 ± 33.8	14.13 ± 3.29

The as-received wire exhibited a significant strength increase (87%) compared to the original Fe-SMA bar, but its ductility decreased dramatically (94%) because of the high cold-working ratio (99% area reduction) during the drawing process. Solution treatment at 1070ºC for 2 hours improved the ductility of the wire substantially; however, both the strength and ultimate strain were still lower compared to the original Fe-SMA bar (27% and 48%, respectively). The additional ageing treatments did not have an effect on the strength of the wires, but they resulted in lower ductility (approximately 40% lower ultimate strains) compared to solution treatment alone.

On the other hand, reducing the annealing temperature below 1070ºC resulted in substantial enhancements with respect to both strength and ductility compared to the as-received condition. In addition, this resulted in greater strengths and comparable ductility with respect to the original Fe-SMA bar. Fig. 3 shows the effect of annealing temperature on the measured tensile properties for specimens that were exposed to a 2-hour solution treatment only (i.e. excluding wires with additional ageing treatments). For the considered heat treatment temperature range, lowering the temperature results in a continuous increase of the peak and offset yield stresses (Fig. 3(a)), reaching maximum tensile strengths up to 1200 MPa at 800ºC (i.e. 30% higher than the original Fe-SMA bar). Ultimate strains are relatively stable within the range of 900ºC-1000ºC and comparable to the original Fe-SMA bar (reductions between 6-12%); however, below 900ºC greater ductility reductions are observed. Nonetheless, the reduced deformation capacity of the wires even at 800ºC is still not detrimental for most structural reinforcement applications, since it is comparable to that of conventional steel reinforcement products.

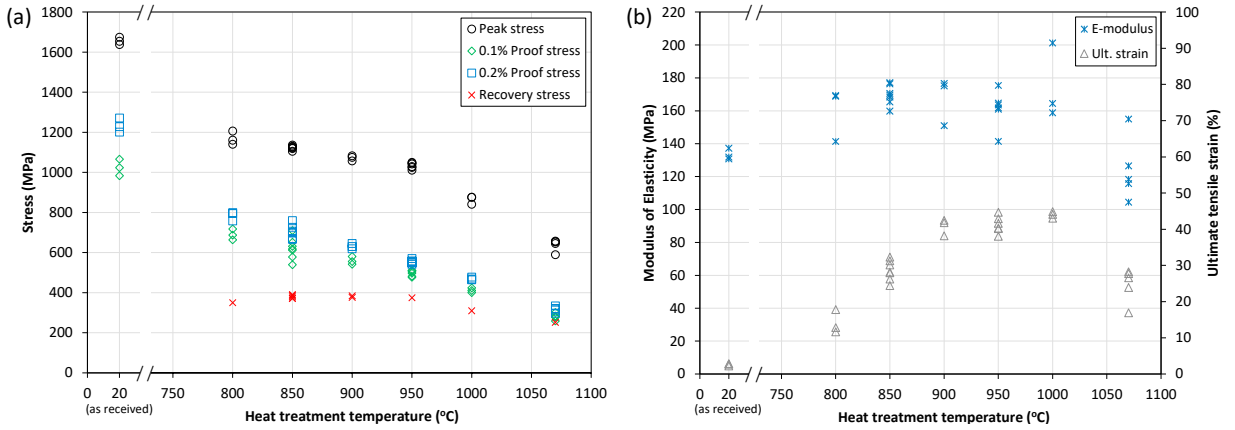

Fig. 3. Variation of tensile properties and recovery stress (at 4% prestrain and activated at 160ºC) with annealing temperature.

3.3. Heated tests for recovery stress activation

Heating of the wires was conducted in an environmental chamber that is fitted on the Zwick/Roell Z020 machine. The activation followed closely the established testing procedure described in Shahverdi et al. (2018), who investigated the mechanical response and recovery stress development in thin cold-rolled strips of the same Fe-SMA alloy. Fig. 4 shows the test setup and the activation procedure. Initially, the wire is loaded in displacement control and ambient temperature up to a target strain level (known as the prestraining stage; shown in Fig. 4(b) for a prestrain of 4%), and then the load is removed (note that the unloading branch of the curve in Fig. 4(b) is non-linear due to pseudoelasticity). Prestraining is performed to induce the formation of the ε-martensite phase in the originally γ-austenite alloy by stressing. For the activation step, a small tensile preload is first applied on the specimen to avoid compression at the early stages of heating due to thermal expansion, before shape memory is activated. After preloading, the specimen is held at constant strain, heated up to the target temperature and cooled back to room temperature, in order to measure the recovery stress development under restrained conditions.

The applied heating and cooling rates were 2°C/min, whereas the holding time at the target temperature was 5 minutes, to ensure uniform temperature within the cross-section and across the full wire length. Target temperatures of 120°C, 160°C, and 195°C were considered herein, similarly to Shahverdi et al. (2018). The wire activation procedure closely followed the established procedure, with the only deviation being the strain control during heating. For typical tensile Fe-SMA specimens the strain is held constant throughout the heating and cooling cycles using a temperature-compensated extensometer. In the case of the thin wire geometry considered herein this was not possible, because the available clip-on extensometer was causing lateral instability (buckling) on the wires at low loads and thus the machine could not maintain control of the crosshead displacement. The automatic extensometer shown in Fig. 2(a) was used only for prestraining the wires, and was removed before the heating because it is not temperature-compensated. Therefore, instead of holding the strain constant based on extensometer readings, the total wire extension was kept constant throughout the activation stage by holding the crosshead displacement increment to zero. For this reason, the test length of the specimens was 300 mm (Fig. 4(a)) to maximize the grip separation inside the chamber and minimize the effects of thermal expansion from heat transfer into the machine's loading rods. Furthermore, another holding step was added at constant displacement for 2 hours after the chamber reached 23°C, to record the final recovery stress value on the wire when the whole system inside the chamber (wire specimen and gripping assembly) has fully cooled down to ambient temperature.

Fig. 5(a) shows the obtained stress versus temperature responses for the case of the wires that were heat-treated at 850°C and for a 4% prestrain. Similar curves were obtained also for the other treatments and prestrain levels. As the temperature increases, the stress reduces initially due to the restrained thermal expansion of the wire. Above approximately 45°C the stress reduction rate decreases due to the initiation of shape recovery in the alloy. During the cooling cycle, thermal strains are recovered and the stress development follows an approximately parallel path to the heating portion of the curve prior to shape memory activation (i.e. 23°C-~45°C). After the temperature inside the chamber reaches 23°C, the stress continues to increase slightly with time, because of the high thermal inertia of the bulky gripping assembly and the respective lag in recovering thermal expansion compared to the thin wire cross-section. Therefore, the fully developed recovery stress is taken as the peak stress value when it stabilizes during the additional 2-hour hold step at 23°C, i.e. when the whole assembly has cooled down and all thermal strain components are fully recovered.

Fig. 5(b) provides an overview of the measured recovery stresses at varying prestrain levels and at different activation temperatures, for wires that were previously heat-treated at 1070°C (with and without ageing treatment); data from wires that were heat-treated at 850°C are also plotted but only for the 160°C activation temperature. The remaining wire conditions were tested for recovery stress only at a 4% prestrain and 160°C activation temperature. The variation of recovery stress with respect to the annealing temperature is included in Fig. 3(a) for comparison with the variation of tensile properties. Fig. 5(b) shows that the recovery stress does not vary considerably with prestrain level in the range of 2%-8%; however, the lower recovery stresses at 1.5% prestrain indicate partial stress-induced martensite formation, and are in agreement with previous findings from strips (Shahverdi et al., 2018). With respect to the annealing temperature (Fig. 3(a)), the recovery stress is enhanced when this is reduced from 1070°C to 950°C, whereas it seems to stabilize in the range of 850°C-950°C, and decreases upon further reduction to 800°C. The best condition combining high tensile properties and the highest recovery stress seems to be that of 850°C.

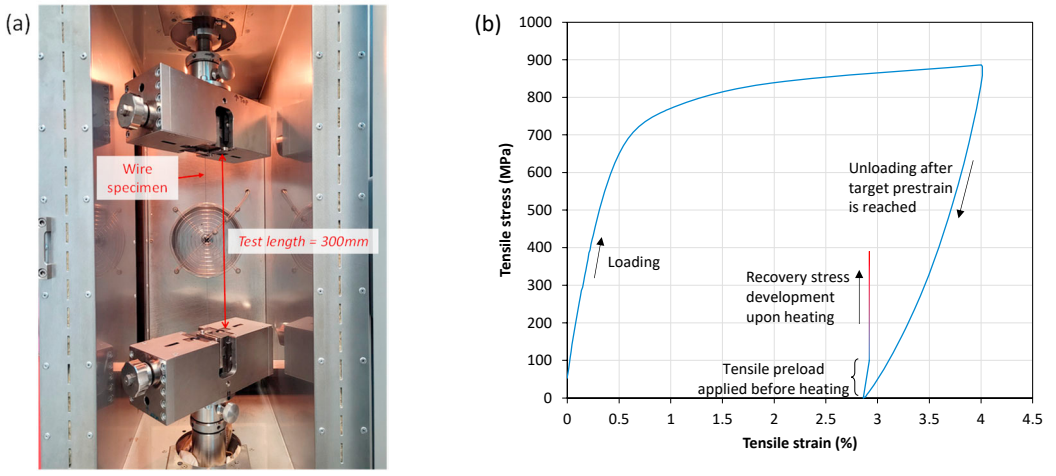

Fig. 4. (a) Tensile setup for activation of recovery stress in the thermal chamber; (b) procedure of prestraining and recovery stress development.

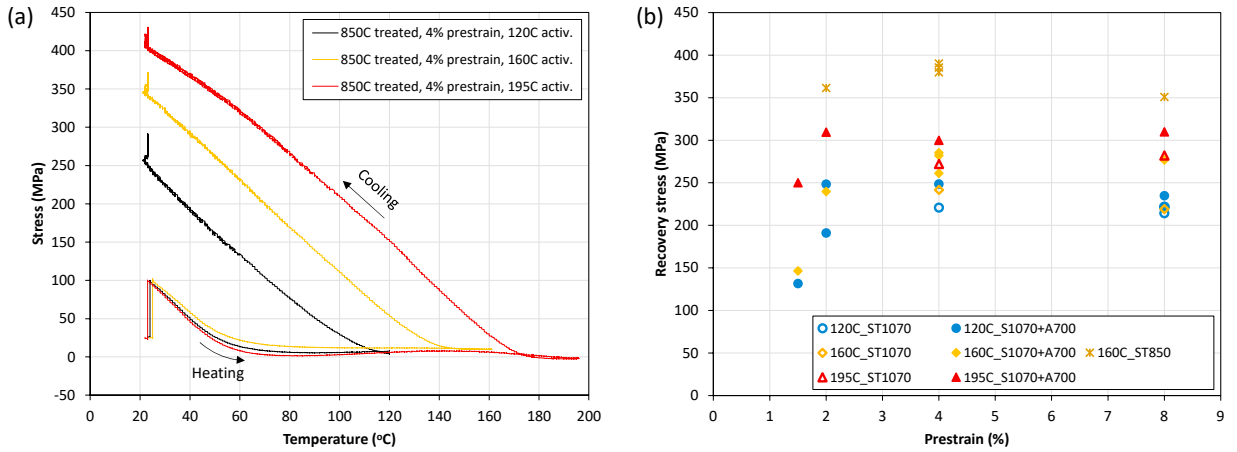

Fig. 5. (a) Recovery stress development of the 850°C-treated wire for 4% prestrain; (b) Effect of prestrain on recovery stress for different wire treatments and activation temperatures.

4. Conclusions and future work

This study introduced a newly developed wire made of iron-based SMA with a diameter of 0.5 mm, and presented an initial study regarding its tensile response and prestressing characteristics. An initial investigation was performed to identify the best-performing conditions of heat-treating the heavily strain-hardened wire to improve its microstructure and recover the ductility losses from the wire drawing process, while maintaining high levels of tensile strength and recovery stress. The optimal performance amongst the conditions considered herein was achieved by heating the wire to 850°C for 2 hours, resulting in a tensile strength of 1117 MPa (26% higher than the original Fe-SMA bar from which the wire was drawn, while still maintaining substantial ductility) and a recovery stress up to 390 MPa (at 160°C activation temperature). Besides the presented macroscopic mechanical characterization, microstructural investigations are currently ongoing to examine the effect of cold drawing and heat treatment on the wire performance by means of scanning electron microscopy and X-ray diffraction analysis.

The observed tensile and prestressing performance of the Fe-SMA wire indicate the strong potential as a candidate material for flexible continuous or dispersed prestressing reinforcement in concrete structures. Future work will focus on investigating its feasibility as a confining spiral wrap and as short fiber reinforcement for concrete, as a cost-effective alternative to the existing NiTi-based wire solutions.

Acknowledgements

The authors would like to express their gratitude to the Ernst Göhner Foundation, re-fer AG, and the Structural Engineering Research Laboratory of Empa for providing financial and technical support for this research study.

References

Aslani, F., Liu, Y. & Wang, Y. (2019). "The effect of NiTi shape memory alloy, polypropylene and steel fibres on the fresh and mechanical properties of self-compacting concrete", *Construction and Building Materials,* 215, 644-659.

Choi, E., Chung, Y.-S., Choi, D.-H. & DesRoches, R. (2012). "Seismic protection of lap-spliced RC columns using SMA wire jackets", *Magazine of Concrete Research,* 64(3), 239-252.

Choi, E., Nam, T.-H., Yoon, S.-J., Cho, S.-K. & Park, J. (2010). "Confining jackets for concrete cylinders using NiTiNb and NiTi shape memory alloy wires", *Physica Scripta,* 2010(T139), 014058.

Deng, Z., Li, Q. & Sun, H. (2006). "Behavior of concrete beam with embedded shape memory alloy wires", *Engineering Structures,* 28(12), 1691-1697.

Dong, Z., Klotz, U. E., Leinenbach, C., Bergamini, A., Czaderski, C. & Motavalli, M. (2009). "A Novel Fe-Mn-Si Shape Memory Alloy With Improved Shape Recovery Properties by VC Precipitation", *Advanced Engineering Materials,* 11(1-2), 40-44.

Gholampour, A. & Ozbakkaloglu, T. (2018). "Understanding the compressive behavior of shape memory alloy (SMA)-confined normal- and high-strength concrete", *Composite Structures,* 202, 943-953.

Krstulovic-Opara, N. & Naaman, A. E. (2000). "Self-Stressing Fiber Composites", *ACI Structural Journal,* 97(2).

Krstulovic-Opara, N. & Thiedeman, P. D. (2000). "Active Confinement of Concrete Members with Self-Stressing Composites", *ACI Materials Journal,* 97(3).

Kumar, P. K. & Lagoudas, D. C. (2008). "Introduction to Shape Memory Alloys", *Shape Memory Alloys: Modeling and Engineering Applications*. Springer US, Boston, MA.

Lee, J.-H., Lee, K.-J. & Choi, E. (2018a). "Flexural capacity and crack-closing performance of NiTi and NiTiNb shape-memory alloy fibers randomly distributed in mortar beams", *Composites Part B: Engineering,* 153, 264-276.

Lee, K.-J., Lee, J.-H., Jung, C.-Y. & Choi, E. (2018b). "Crack-closing performance of NiTi and NiTiNb fibers in cement mortar beams using shape memory effects", *Composite Structures,* 202, 710-718.

Li, H., Liu, Z.-q. & Ou, J.-p. (2006). "Behavior of a simple concrete beam driven by shape memory alloy wires", *Smart Materials and Structures,* 15(4), 1039.

Maji, A. K. & Negret, I. (1998). "Smart Prestressing with Shape-Memory Alloy", *Journal of Engineering Mechanics,* 124(10), 1121-1128.

Mas, B., Biggs, D., Vieito, I., Cladera, A., Shaw, J. & Martínez-Abella, F. (2017). "Superelastic shape memory alloy cables for reinforced concrete applications", *Construction and Building Materials,* 148, 307-320.

Mas, B., Cladera, A. & Ribas, C. (2016). "Experimental study on concrete beams reinforced with pseudoelastic Ni-Ti continuous rectangular spiral reinforcement failing in shear", *Engineering Structures,* 127, 759-768.

Menna, D. W., Genikomsou, A. S. & Green, M. F. (2023). "Flexural performance and crack closing capacity of double-hooked-end superelastic shape memory alloy fibre-reinforced concrete beams under cyclic loading using digital image correlation", *Construction and Building Materials,* 409, 133744.

Moser, K., Bergamini, A., Christen, R. & Czaderski, C. (2005). "Feasibility of concrete prestressed by shape memory alloy short fibers", *Materials and Structures,* 38(5), 593-600.

Ozbulut, O. E., Daghash, S. & Sherif, M. M. (2016). "Shape Memory Alloy Cables for Structural Applications", *Journal of Materials in Civil Engineering,* 28(4), 04015176.

Raza, S., Shafei, B., Saiid Saiidi, M., Motavalli, M. & Shahverdi, M. (2022). "Shape memory alloy reinforcement for strengthening and self-centering of concrete structures—State of the art", *Construction and Building Materials,* 324, 126628.

Reedlunn, B., Daly, S. & Shaw, J. (2013). "Superelastic shape memory alloy cables: Part I – Isothermal tension experiments", *International Journal of Solids and Structures,* 50(20), 3009-3026.

Rius, J. M., Cladera, A., Ribas, C. & Mas, B. (2019). "Shear strengthening of reinforced concrete beams using shape memory alloys", *Construction and Building Materials,* 200, 420-435.

Shahverdi, M., Michels, J., Czaderski, C. & Motavalli, M. (2018). "Iron-based shape memory alloy strips for strengthening RC members: Material behavior and characterization", *Construction and Building Materials,* 173, 586-599.

Sherif, M. M., Tanks, J. & Ozbulut, O. E. (2017). "Acoustic emission analysis of cyclically loaded superelastic shape memory alloy fiber reinforced mortar beams", *Cement and Concrete Research,* 95, 178-187.

Shin, M. & Andrawes, B. (2010). "Experimental investigation of actively confined concrete using shape memory alloys", *Engineering Structures,* 32(3), 656-664.

Shin, M. & Andrawes, B. (2011). "Lateral Cyclic Behavior of Reinforced Concrete Columns Retrofitted with Shape Memory Spirals and FRP Wraps", *Journal of Structural Engineering,* 137(11), 1282-1290.

Wang, S., Mohri, M., Li, L., Izadi, M., Jafarabadi, A., Pichler, N. & Ghafoori, E. (2023). "Memory-Steel for Smart Steel Structures: A Review on Recent Developments and Applications", *ce/papers,* 6(3-4), 949-958.

Yang, Y., Arabi-Hashemi, A., Leinenbach, C. & Shahverdi, M. (2021). "Influence of thermal treatment conditions on recovery stress formation in an FeMnSi-SMA", *Materials Science and Engineering: A,* 802, 140694.